Metallogr. Microstruct. Anal. (2012) 1:35–44
DOI 10.1007/s13632-012-0011-2

TECHNICAL ARTICLE

Role of Rhenium on Solidification, Microstructure, and Mechanical Properties of Standard Alloy 718

Nader El-Bagoury · Adel A. Omar · K. Ogi

Received: 29 November 2011 / Accepted: 14 February 2012 / Published online: 20 March 2012

Abstract The effect of Rhenium (Re) additions to Standard Alloy 718 on solidification, microstructure, and mechanical properties represented by hardness was studied. Re has a very high strain hardening rate, which is about 3.5 times than that of W or Mo. Re retards γ'' and γ' coarsening, and also forms clusters within the γ matrix. In addition, Re does not from carbides. However, the microstructure of Re-containing Alloy 718 has a higher volume fraction of δ phase than the standard alloy. Electron microprobe analysis and transmission electron microscopy observations were used to identify the precipitation of hard γ'' and γ' phases as well as δ phase. Re elevates phase transformation temperatures of γ matrix, eutectic γ/NbC, and eutectic γ/Ni_2Nb. The volume fractions of γ dendrites, NbC and Ni_2Nb phases, are increased with Re content in Alloy 718. Enhancement of hardness was also evident in the vicinity of a Re-cluster.

N. El-Bagoury (✉)
Central Metallurgical Research and Development Institute (CMRDI), P.O. Box 87, Helwan, Cairo, Egypt
e-mail: nader_elbagoury@yahoo.com

N. El-Bagoury
Chemistry Department, Faculty of Science, Taif University, El-Haweyah, P.O. Box 888, E-Taif, Saudi Arabia

A. A. Omar
Mechanical Engineering Department, College of Engineering, Taif University, Taif, Saudi Arabia

A. A. Omar
Mechanical Engineering Department, Benha Faculty of Engineering, Benha University, Benha, Egypt

K. Ogi
Department of Materials Processing Engineering, Kyushu University, 744 Motooka, Nishi-Ku, Fukuoka 819-0395, Japan

Keywords Standard Alloy 718 · Rhenium · Casting · Laves and delta phases · Mechanical properties

Introduction

The strength of the commercial superalloys arises from a combination of hardening mechanisms, including contributions from solid solution elements, precipitates, and grain size. Solid solution hardening is a powerful method to improve the mechanical properties of this type of alloy. Ni base superalloys contain substantial alloying elements in solid solution to provide strength, creep resistance, and resistance to surface degradation. After suitable heat treatment processes, further hardening is provided by coherent stable intermetallic compounds such as γ' $\{Ni_3(Al, Ti)\}$ and γ'' $Ni_3(Nb)$ [1].

The mechanical properties of Ni base superalloys have been optimized, especially the creep resistance, by introducing large amounts of refractory alloying elements such as W, Ta, and Mo. Additions of Rhenium (Re) up to 6.0% to single crystal Ni base superalloys have been made [2]. Re, as a pure metal, has a higher strength and superior modulus of elasticity in comparison with Mo, Nb, W, and Ta [3–6]. Moreover, Re significantly retards the coarsening rate of γ' phase at high temperatures or during heat treatment [7]. As with the four refractory metals, Re has a strong preference for occupying the Al sites in γ' (Ni_3Al,) increasing the γ' volume fraction. Additions of Re to Ni base superalloys is beneficial in producing alloys with a small negative lattice misfit parameter [8, 9]. Atom probe investigations of Re-containing superalloys have reported pileup of Re at the γ/γ' interface. Re has a unique phenomenon among other alloying elements by forming clusters within the γ matrix. These

Table 1 Chemical composition of ST and Re-containing Alloy 718 (mass%)

Alloy %	C	Nb	Ti	Cr	Fe	Ni	Mo	Al	Re
ST Alloy 718	0.06	4.88	0.95	19.45	18.39	52.65	3.06	0.56	…
$Re^{2.4}$ Alloy 718	0.059	4.76	0.93	18.98	17.83	51.39	2.99	0.55	2.40
$Re^{3.5}$ Alloy 718	0.058	4.71	0.92	18.77	17.63	50.81	2.95	0.54	3.50
$Re^{6.0}$ Alloy 718	0.056	4.59	0.89	18.28	17.17	49.49	2.88	0.53	6.00

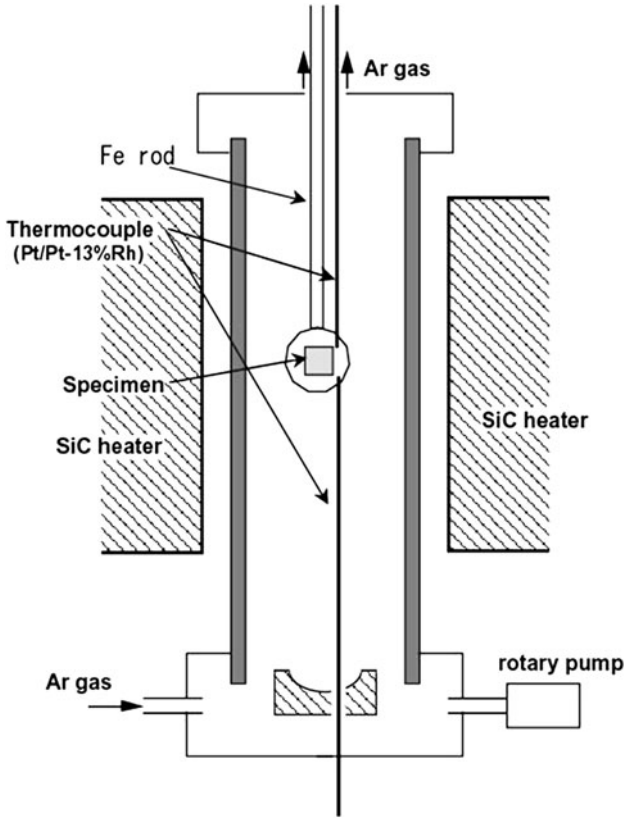

Fig. 1 Experimental apparatus used in the study of solidification process

clusters are thought to be a more potent source of strengthening than other elements in solid solution [10–14].

In this study, we set out to improve the mechanical properties of Alloy 718 alloy by adding various amounts of Re. Also, the influence of different heat treatment processes on the mechanical properties of Alloy 718 was investigated.

Experimental Procedures

Chemical Composition and Melting Process

The chemical compositions shown in Table 1 were used for production of (ST) and three Re-containing Alloy 718 master alloys.

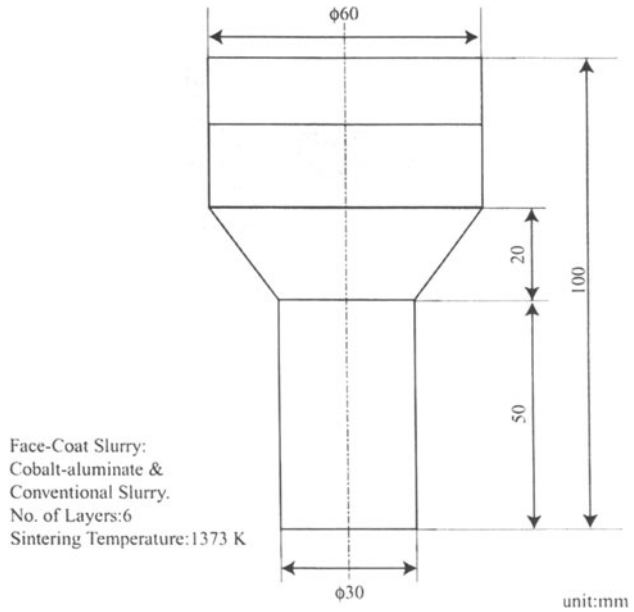

Fig. 2 Dimensions of the ceramic mold

The melting process was accomplished in a graphite resistance electric furnace under argon atmosphere. The study of solidification for both ST and Re-containing Alloy 718 heats was carried out using experimental apparatus shown in Fig. 1, by remelting about 30 g of each alloy. The melt was cooled down to a predetermined temperature (~40 °C superheat for all alloys) and subsequently poured into a preheated ceramic mold under air atmosphere. The mold preheating temperature was kept at 1373 K in all cases. This ceramic mold was composed of face-coat slurry containing cobalt aluminate ($CoO–Al_2O_3$). Dimensions of the ceramic mold are provided in Fig. 2.

Microstructure Investigation

An Electron Probe Microanalyzer (EPMA) and a Light Microscope (LM), fitted with a digital camera, were used to investigate the phases present in the microstructure [γ, carbides, and laves and delta (δ) phases]. The specimens were prepared by standard metallographic procedures and etched in 10% oxalic acid. EPMA was used to confirm the precipitation of δ phase. Both super back-scattered electron (SBSE) and reflected electron (RE) images were used for

recognizing and differentiating between various phases such as Ni_2Nb (laves), NbC, and δphase.

Differential Scanning Calorimetry (DSC)

DSC measurements were performed using a Netzch STA 449 F3 Jupiter instrument to examine the crystallization behavior of standard and experimental alloys. Prior to the testing of the specimen, the DSC unit was calibrated with high purity indium (99.99 pct) at a heating rate of 10 °C/min.

Transmission Electron Microscopy

Selected samples were prepared for transmission electron microscopy. The TEM was operated at 1,000 kV and equipped with a tilt rotation probe holder. After the aging treatment, the samples were mechanically ground to ~80 μm thickness, then electro-polished using at room temperature in a bath containing a chemical solution of 70% dimethyl ether ($C_2H_5OC_2H_5$), 20% ethanol (C_2H_5OH), and 10% perchloric acid ($HClO_4$), at <15 V.

Hardness Measurements

Hardness measurements are very important in this kind of research because hardness and tensile strength are related to each other and to the microstructure. Therefore, Vickers hardness was measured under a load of 30 kg. The mean value over ten measurements was evaluated.

Results and Discussion

Microstructure of As-Cast ST and Re-Containing Alloy 718

The solidification sequence for ST Alloy 718 is illustrated in Fig. 3. The microstructure consists of primary γ and eutectic (γ + NbC), and eutectic (γ + Ni_2Nb). Figure 4 shows as-cast microstructures of the three experimental Re alloys.

EPMA micrographs, SBSE and RE images, are used to distinguish NbC from Ni_2Nb, as shown in Fig. 5 for 6.0%

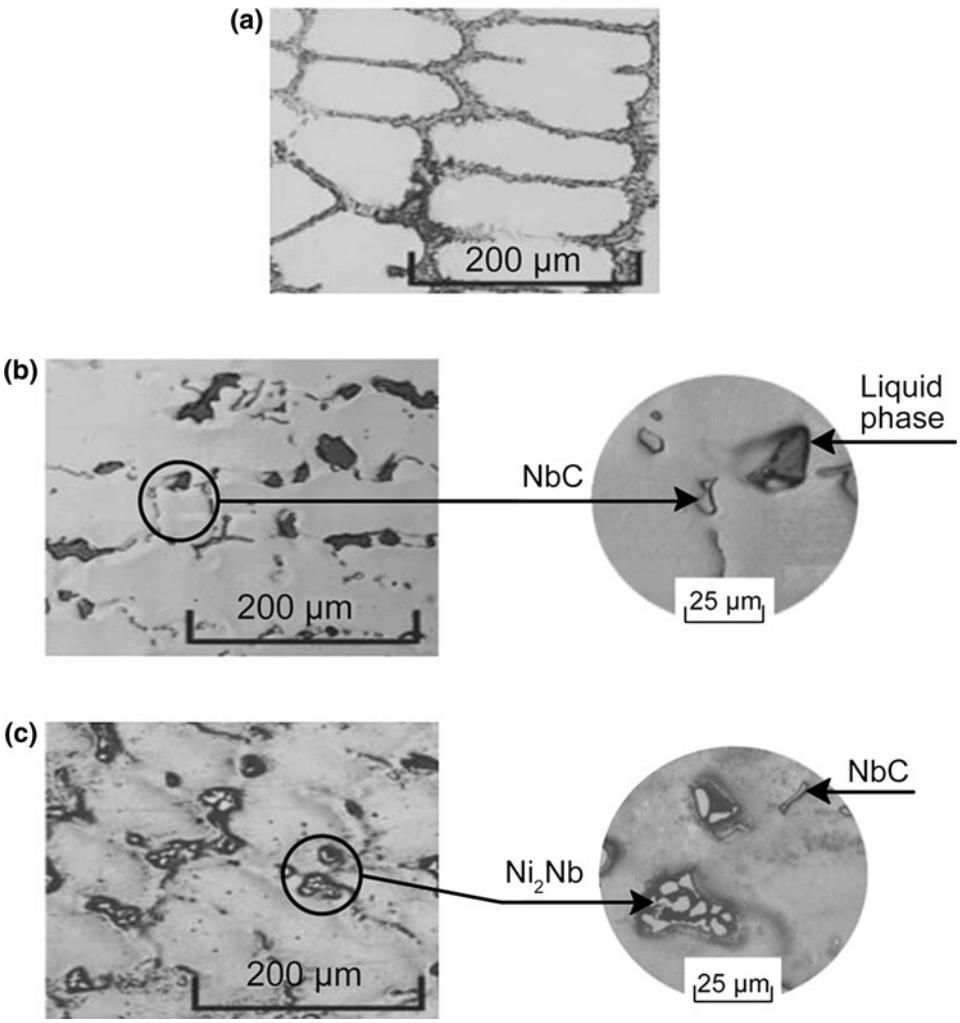

Fig. 3 Solidification sequence of **a** primary γ matrix and residual quenched liquid in as cast ST Alloy 718, **b** primary γ, eutectic γ/NbC, and quenched liquid in as-cast ST Alloy 718, and **c** primary γ, eutectic γ/NbC, and eutectic γ/laves in as cast ST Alloy 718

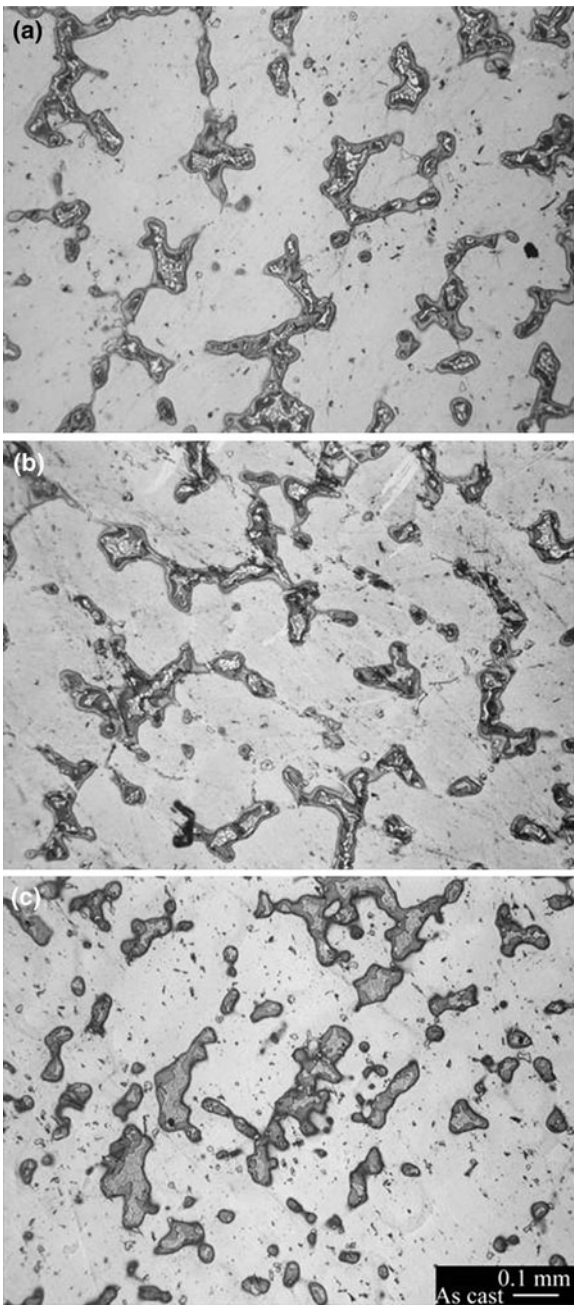

Fig. 4 Microstructure of as-cast Re-containing alloys. **a** 2.4% Re Alloy 718, **b** 3.5% Re Alloy 718, and **c** 6.0% Re Alloy 718

Re alloy. The γ phase solidifies as dendrites, as shown in Fig. 6 for the case of 2.4% Re alloy.

Both the eutectic (γ/NbC) and the eutectic (γ/Ni_2Nb) were found to form later in the last stages of the solidification process in the interdendritic regions, as shown in Fig. 7(a) and (b) for the 6.0 and 3.5% Re alloys, respectively. After completion of the solidification process for the as-cast 2.4% Re alloy, the microstructure consists of the same phases: γ matrix and eutectic (γ/NbC) and eutectic (γ/Ni_2Nb), as shown in Fig. 7(c).

Table 2 represents the volume fractions of γ matrix, eutectic (γ/NbC), and eutectic (γ/Ni_2Nb) in ST and Re-containing alloys. These measurements of the volume fraction of were carried out using at least 10 SBSE and RE images, which assisted in differentiation between NbC and Ni_2Nb phases, as shown in Fig. 5. From these measurements, it can be concluded that the volume fraction of γ matrix is enlarged at the expense of both eutectic (γ/NbC) and eutectic (γ/Ni_2Nb) by Re additions. This can be attributed to the fact that Re as an alloying element segregates into γ dendrites and not to the eutectic [15]. Consequently, dendritic volume fraction increases.

The effect of Re addition on the volume fraction of NbC and Ni_2Nb phases in the two eutectics can be found in Table 3. NbC and Ni_2Nb phases are enriched in the

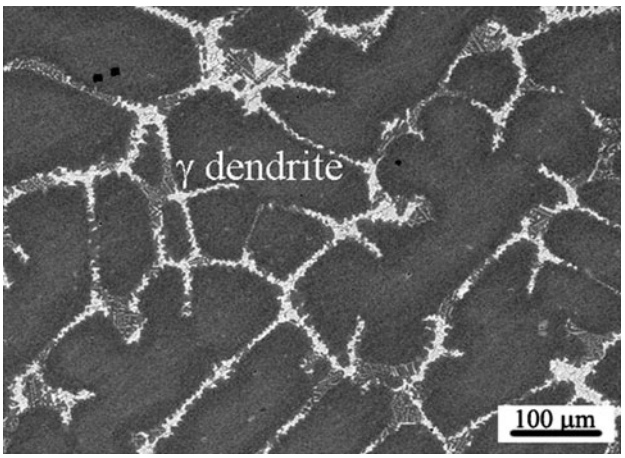

Fig. 6 As-cast 2.4% Re Alloy 718, primary γ dendrites and residual quenched liquid

Fig. 5 Microstructure of 6.0% Re Alloy 718. **a** SBSE and **b** RE

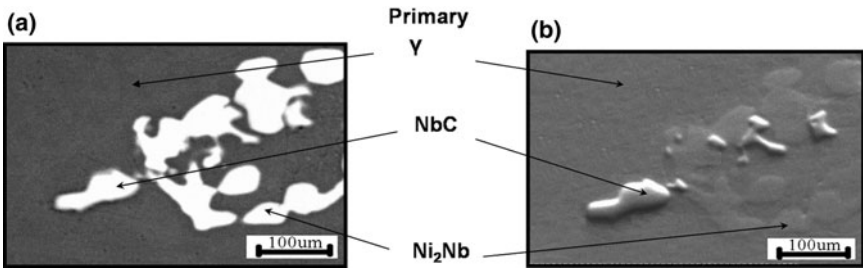

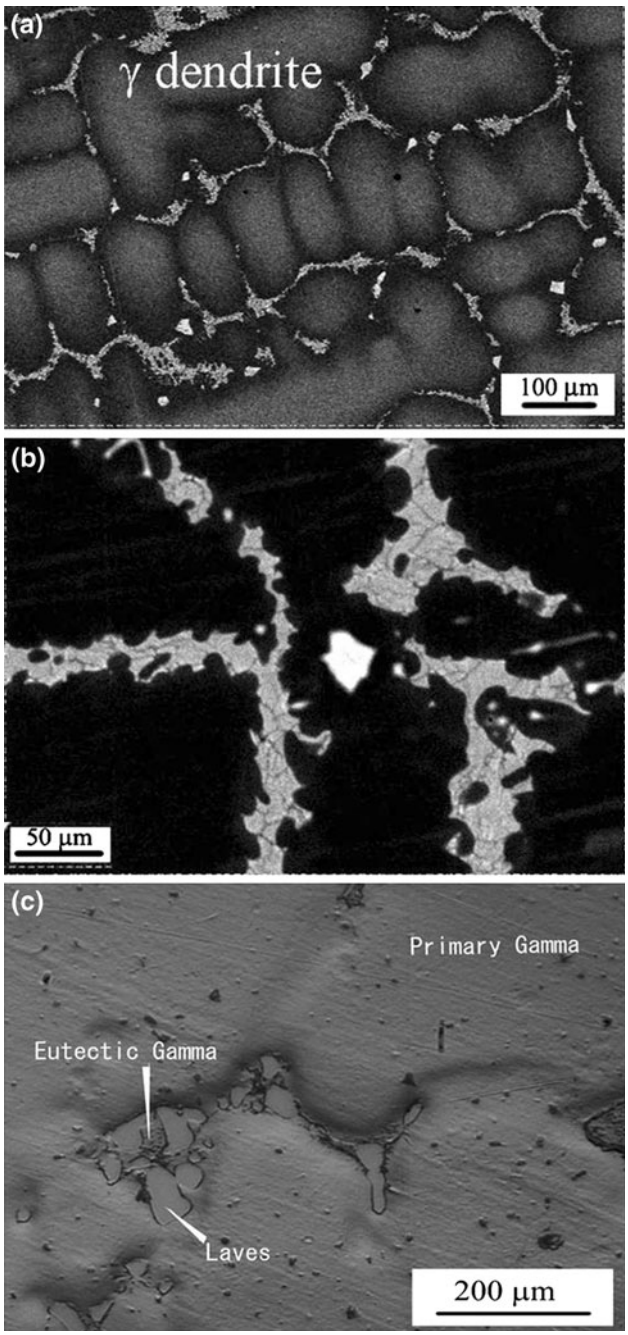

Fig. 7 Microstructure of **a** primary γ matrix and residual quenched liquid in as cast 6.0% Re Alloy 718, **b** primary γ, eutectic γ/NbC, and quenched liquid in as-cast 3.5% Re Alloy 718, and **c** primary γ, eutectic γ/NbC, and eutectic γ/laves in as-cast 2.4% Re Alloy 718

Table 2 Volume fractions of different phases in Alloy 718

Alloy	γ Dendrites	Eu (γ/NbC)	Eu (γ/Ni_2Nb)
ST Alloy 718	70.90	20.22	8.88
$Re^{2.4}$ Alloy 718	77.21	16.07	6.72
$Re^{3.5}$ Alloy 718	79.08	15.09	5.83
$Re^{6.0}$ Alloy 718	82.50	13.35	4.15

eutectics as Re content increases in the respective alloys. This increment in % of NbC and Ni_2Nb phases in the eutectic is due to Re replacement of Nb in the γ dendrites. Re forces Nb to segregate into interdendritic regions where the eutectic (γ/NbC) and eutectic (γ/Ni_2Nb) are formed. Consequently, NbC and Ni_2Nb volume fractions in each eutectic increase by increasing the Nb content in the interdendritic regions.

Delta phase precipitates on the surface of Ni_2Nb as a needle-like shape in six Re alloy, as shown in Fig. 8. This phase precipitates after the solidification is complete. The δ phase forms as a solid-state transformation.

EPMA Microanalysis of Different Phases in Alloy 718 Alloys

Figure 9 shows the relationship between the Re content in Re-containing Alloy 718 and the Re percentages in different phases. As the Re alloy content increases, the Re percentage in all phases such as eutectic γ (Ni_2Nb), Ni_2Nb, and eutectic γ (NbC) increases, except for NbC. In eutectic (γ/Ni_2Nb), Re prefers to segregate into Ni_2Nb rather than eutectic γ, as shown in Fig. 9, in the case of eutectic (γ/NbC), Re diffuses to eutectic γ at the expense of NbC.

Table 3 Percentages of NbC and Ni_2Nb in eutectics

Alloy	%NbC Eu (γ/NbC)	%Ni_2Nb Eu (γ/Ni_2Nb)
ST Alloy 718	5.76	31.25
$Re^{2.4}$ Alloy 718	7.56	35.37
$Re^{3.5}$ Alloy 718	8.15	40.48
$Re^{6.0}$ Alloy 718	9.29	53.49

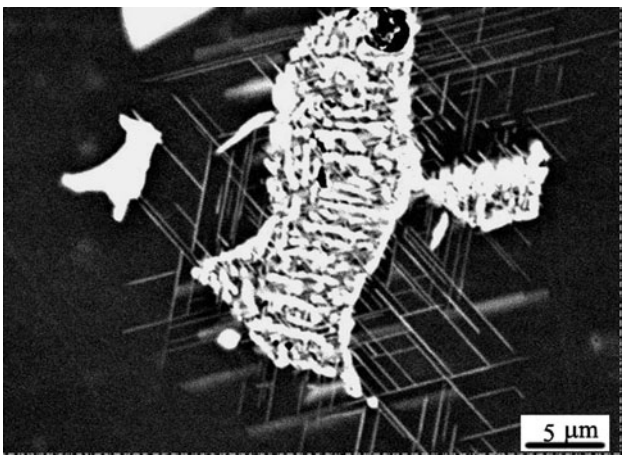

Fig. 8 Delta phase precipitated as a needle-like shape at the circumference of Ni_2Nb laves phase

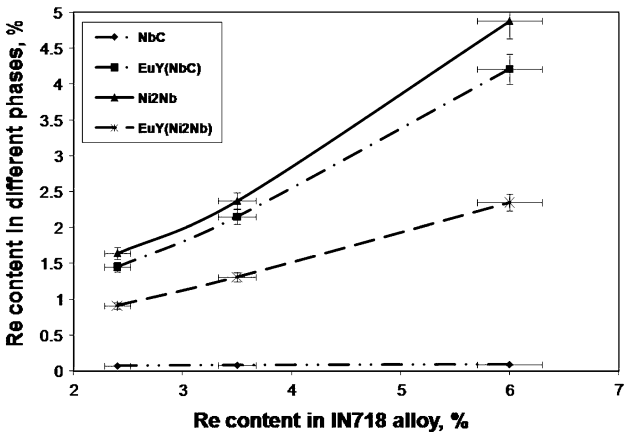

Fig. 9 Re content in different phases in Re-containing Alloy 718

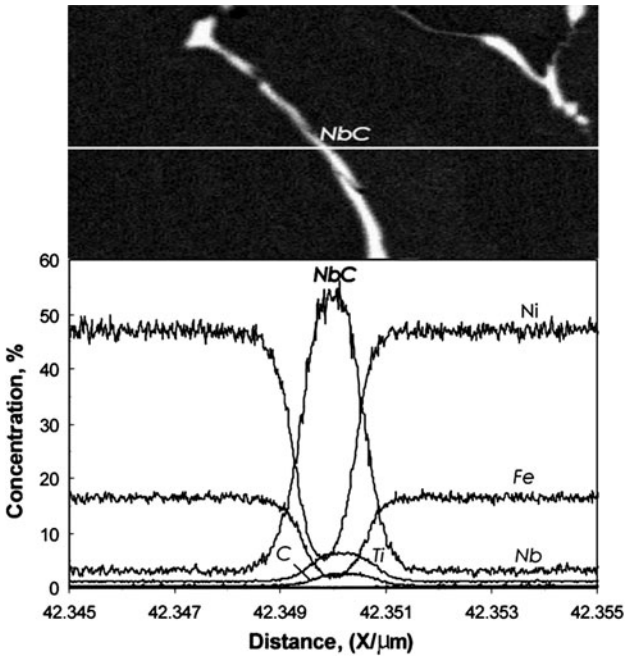

Fig. 10 Line analysis through NbC in ST Alloy 718

Figures 10 and 11 illustrate the line analysis of NbC and δ phase in ST and 3.5% Re alloys, respectively. As shown in Fig. 10, NbC carbides also contain some Ti in the ST alloy.

Delta phase is enriched in Ni and Nb contents in comparison with the surrounding eutectic γ. However, the concentration of Fe is lower in δ phase.

DSC Measurements

A DSC technique is commonly used to follow microstructural changes such as precipitation reactions in superalloys. DSC measurements were carried out on the Standard (ST) 2.4 and 6.0% Re alloys at a constant heating rate of 10 °C/min. Figure 12 shows a DSC

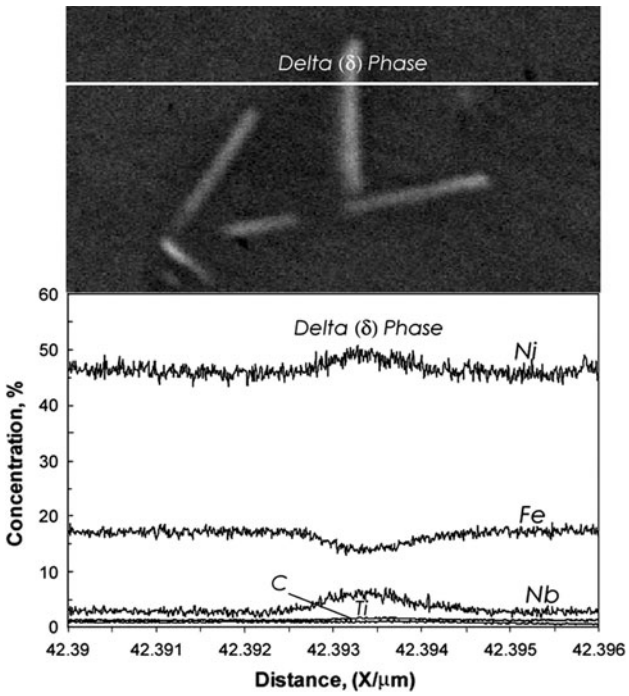

Fig. 11 Line analysis through δ phase in 3.5% Re Alloy 718

heating trace with various endotherms/exotherms. Five peaks of interest are highlighted in this figure. A broad melting interval which is the first peak at 1377.2 °C represents the melting of γ matrix for the ST alloy. This melting temperature is increased to 1380.2 and 1387.0 °C for 2.4 and 6.0% Re-containing alloys, respectively. The second peak at 1321.7 °C corresponds to the dissolution of eutectic (γ/NbC) for ST Alloy 718 alloy. This peak is elevated to 1,342 and 1,355°C in the case of 2.4 and 6.0% Re-containing alloys, respectively. The fourth peak indicates the temperature at which the dissolution of eutectic (γ/Ni_2Nb) at 1206.7, 1212.2, and 1210.6 °C is taking place for ST 2.4 and 6.0% Re alloys, respectively. The fifth peak at 1097.5 and 1119.5 °C, which represents the dissolution of δ phase in ST and 2.4% Re alloys, respectively. The last two peaks represent the dissolution of γ' and γ'' precipitates. All these phase transformations with heating are summarized in Table 4. The endothermic peak at 1337.5 °C might be dissolution of a metastable phase or a relaxation effect.

Only in 2.4 and 6.0% Re alloys, two peaks at 1304.7 and 1307.2 °C, respectively, were considered to be related to the dissolution of Re clusters.

TEM Microstructural Investigation

Figure 13 shows a bright field review of the as cast of 3.5% Re alloy. This figure illustrates precipitation of hard γ' and γ'' phases.

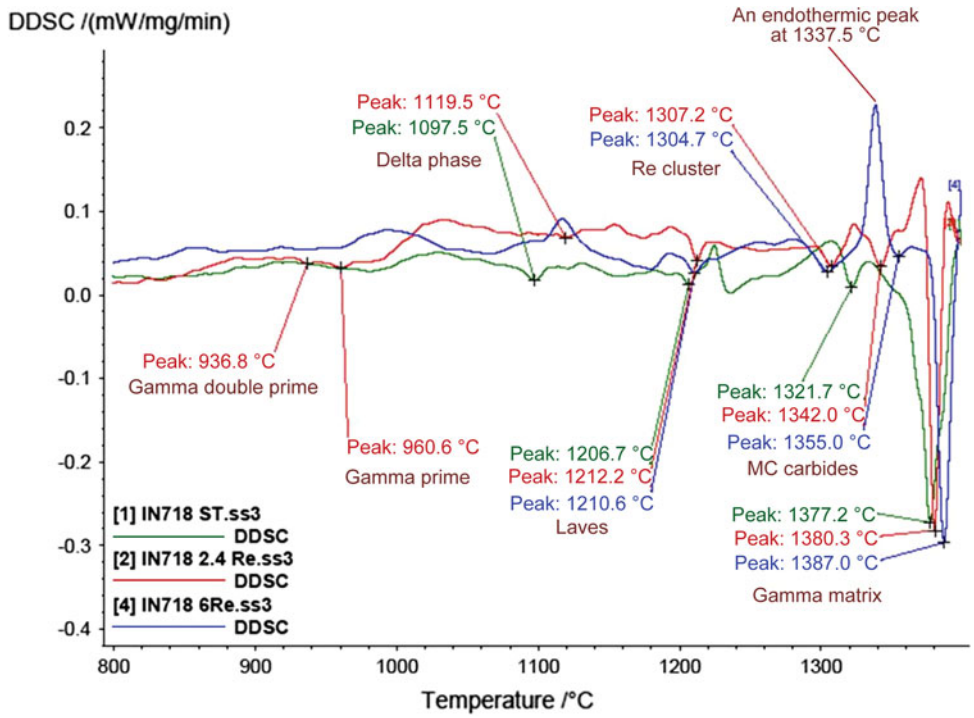

Fig. 12 DSC heating curve for ST 2.4 and 6.0% Re-containing Alloy 718

Table 4 DSC measurements of dissolution/melting temperatures of different phases in ST and Re alloys

Phase:	γ Matrix	MC	Laves	δ	γ'	γ''	Re cluster
Alloy							
ST Alloy 718	1377.2	1321.7	1206.7	1097.5	903	938	…
$Re^{2.4}$ Alloy 718	1380.3	1342	1212.2	1120.5	936.8	960.6	1304.7
$Re^{6.0}$ Alloy 718	1387.0	1355	1210.6	1133.6	…	…	1307.2

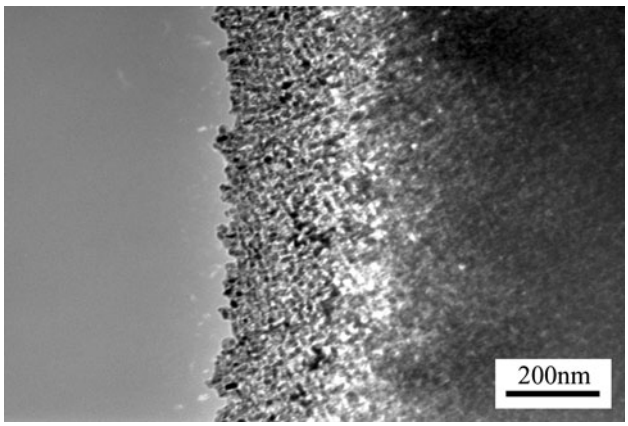

Fig. 13 Bright-field micrograph of 3.5% Re Alloy 718

Figure 14(a) shows the dark field micrograph for γ' precipitates in the as-cast six Re alloy, obtained from an (010) γ' spot, and the precipitates are recognized to appear as spherical particles. [16–19]. Figure 14(b) shows the dark field micrograph obtained from a (1 ½ 0) γ'' spot, which usually appear as long disk-shaped, uniformly distributed in the matrix with a very high density [19, 20].

Figure 15(a) shows the ⟨001⟩ matrix zone axis selected area diffraction (SAD) pattern for the as-cast 2.4% Re alloy. Figure 15(b) demonstrates the key to SAD pattern, {100} and {110} type reflections correspond to both γ' and γ'' phases whereas {1 ½ 0}-type reflections correspond to only γ''.

Changes in Hardness

Hardness gives a good indication of the precipitation state of hard phases such as γ'' and γ'. The hardness of as-cast ST and Re alloys was measured to find out the effect of Re on mechanical properties of ST Alloy 718 alloy. As shown in Fig. 16, the hardness measurements of Re-containing Alloy 718 alloys are higher than that of the ST alloy. As the Re

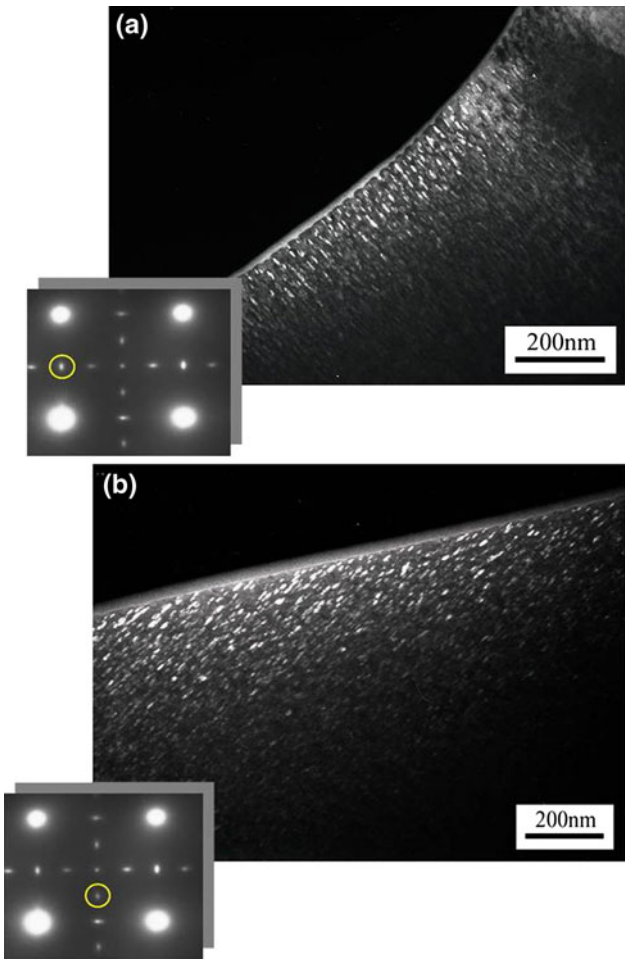

Fig. 14 As-cast 6.0% Re Alloy 718. Dark-field micrograph using **a** (010) γ' spot and **b** (1 ½ 0) γ'' spot

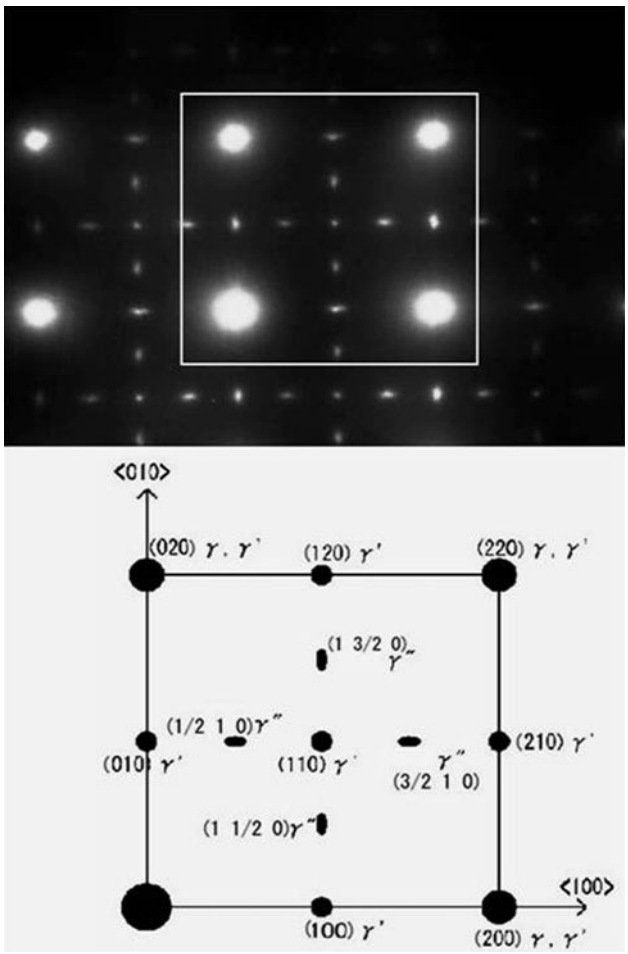

Fig. 15 The diffraction pattern of as-cast 2.4% Re Alloy 718 specimen from {100} matrix zone axis

percentage in as-cast Re increases the hardness value increases.

The hardness value of the ST alloy is 175 HV_{30}, while the hardness measurements for 2.4, 3.5, and 6.0% Re alloys are 208, 216, and 220, respectively. This means that the hardness of ST Alloy 718 is improved by about 18% with the addition of 2.4% of Re. Moreover, this increment in the hardness of ST Alloy 718 is enhanced with increasing Re percentage to 3.5 and 6.0. The hardness enhancement for ST Alloy 718 is increased to 23 and 26% as the Re content raises to 3.5 and 6.0%, respectively.

The hardness measurements of ST and Re-containing alloys are entirely dependent on the hard phases present in the microstructure in addition to their volume fraction and size in that microstructure. The γ'' and γ'' phases are the hard phases that can be found in the microstructure as well as Re clusters formed in the γ matrix [19]. Therefore, the interpretation of increasing hardness for Re-containing 718 alloys could be due to the presence of Re clusters, which are considered to be a more effective source of

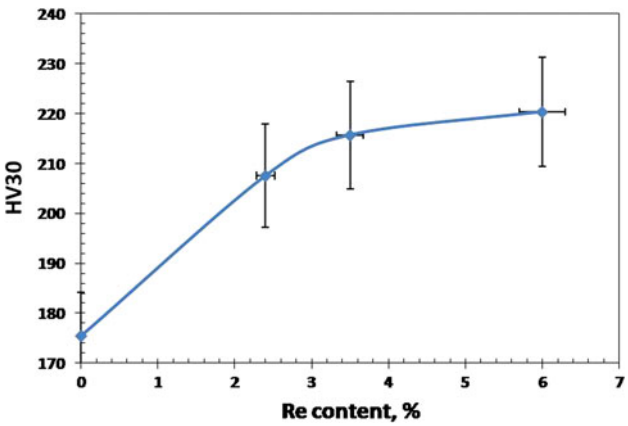

Fig. 16 Hardness measurements versus rhenium content in Alloy 718

strengthening than other elements in solid solution. [16]. Figures 17 and 18 demonstrate the formation of Re clusters, where the pentamer cluster of Re is formed through the combination of five Re atoms. In Fig. 18, a trimer and a

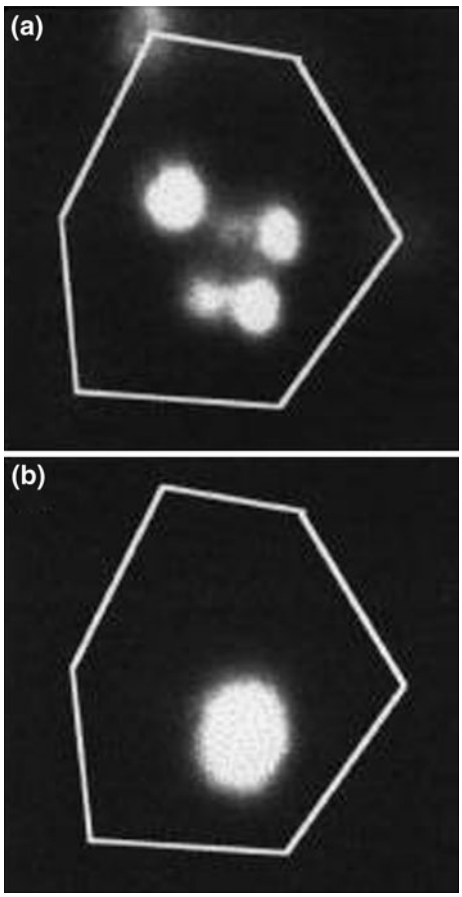

Fig. 17 Formation of rhenium pentamer; five Re atoms (**a**) have combined into one cluster (**b**). Reprinted from Goldstein and Ehrlich [21], p. 111. Copyright 1999, with permission from Elsevier

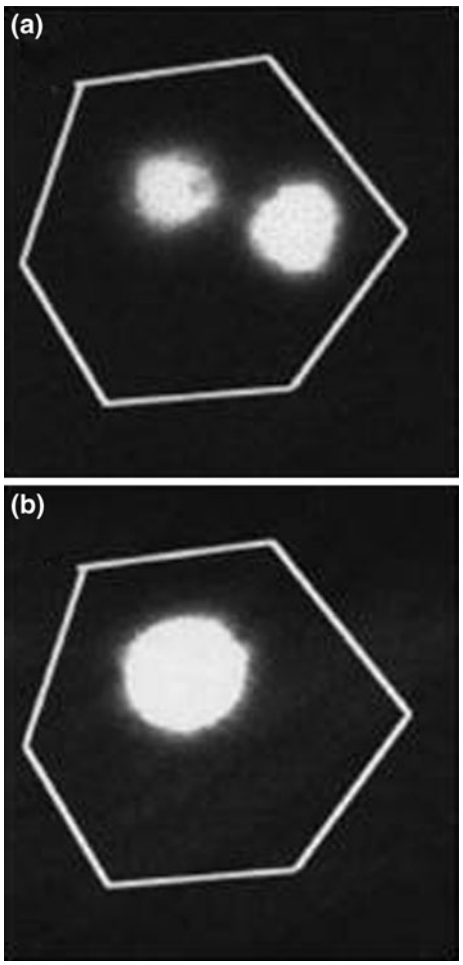

Fig. 18 **a** Separate pentamer and trimer Re cluster. **b** Clusters in (**a**) coalesce into an octamer Re cluster. Reprinted from Goldstein and Ehrlich [21], p. 112. Copyright 1999, with permission from Elsevier

pentamer Re clusters have coalesced to form one octamer Re clusters [21].

Another reason that support the increment of hardness values of Re containing-alloys is that the volume fraction of γ' phase is increased as Re content is increased.

From the above, the hardness of ST Alloy 718 can be enhanced by adding Re as an alloying element to the chemical composition of ST Alloy 718.

Conclusions

1. Re as an alloying element elevates the phase transformation temperatures of the ST Alloy 718, which in turn can expand the applicability of the ST Alloy 718.
2. The microstructure of ST and Re-containing Alloy 718 contains precipitation of δ phase with a needle-shaped morphology surrounding the Ni_2Nb phase.
3. The hardness level of cast ST Alloy 718 is significantly increased with increasing Re content. This can be related to the formation of Re clusters in γ matrix, in addition to increasing the volume fraction of γ' phase in Re-containing alloys.
4. Re increases the volume fraction of γ dendrites at the expense of eutectic γ/NbC and eutectic γ/Ni_2Nb phases. The fraction of Re is increased in different phases as the Re content in Alloy 718 increases, except for the NbC carbide phase.

References

1. T.S. Chester, S.S. Norman, C.H. William, *Superalloys II* (Wiley, New York, 1976)
2. P. Caron, T. Khan, Evolution of Ni-based superalloys for single crystal gas turbine blade applications. Aerosp. Sci. Technol. **3**, 513 (1999)
3. Aerospace Structural Metals Handbook, Code 5201, 1963; Code 5206, 1966; Code 5208, 1967; Code 5209, 1971; Code 5211, 1973; U. S. Department of Defense, Mechanical Properties Data Center

4. H.Y. Zhang, S.H. Zhang, M. Chang, Z.X. Li, Deformation characteristics of δ phase in the delta-processed Inconel 718 alloy. Mater. Charact. **61**(1), 49 (2010)
5. S. Ceresara, M. Ricci, N. Sacchetti, G. Sacerdoti, *Applied Superconductivity Conference, IEEE Transactions on Magnetics*, vol. 11, No. 2, March (1975)
6. R. Bakish (ed.), *Electron Beam Melting and Refining: State of the Art* (Bakish Materials Corporation, Englewood, 1989)
7. A.F. Giamei, D.L. Anton, Rhenium additions to a Ni-base superalloy: effects on microstructure. Met. Trans. **16A**, 1997 (1985)
8. H. Murakami, H. Harada, H.K.D.H. Bhadeshia, The location of atoms in Re- and V-containing multicomponent nickel-base single-crystal superalloys. Appl. Surf. Sci. **7**(6/77), 177 (1994)
9. H. Harada, T. Yamagata, T. Yokokawa, K. Ohno, M. Yamazaki, *Proceedings of the 5th Intranational Conference on Creep and Fracture of Engineering Materials and Structures*, Swansea, UK (1993), p. 255
10. H. Murakami, P. J. Warren, H. Harada, *Proceedings of the 3rd Intranational Charles Parsons Turbine Conference*, Newcastle-Upon-Tyne, England, April 25–27, 1995 (Institute of Materials, London, 1995), p. 343
11. D. Blavette, P. Caron, T. Khan, An atom probe investigation of the role of rhenium additions in improving creep resistance of Ni-base superalloys. Scripta Metall **20**, 1395 (1986)
12. A.T. Egbewande, R.A. Buckson, O.A. Ojo, Analysis of laser beam weldability of Inconel 738 superalloy. Mater. Charact. **61**(5), 569 (2010)
13. D. Blavette, P. Caron, T. Khan, *Proceedings Superalloys*, Seven Springs, Pennsylvania, September 18–22, 1988 (TMS, Warrendale, 1988), p. 305
14. N. Wanderka, U. Glatzel, Chemical composition measurements of a nickel-base superalloy by atom probe field ion microscopy. Mater. Sci. Eng., A **203**, 69 (1995)
15. D. Mukhreji, P. Strunz, D. Del Genovese, R. Gilles, J. Roesler, A. Wiedenmann, Metall. Mater. Trans. A **34A**, 2781 (2003)
16. G.A. Rao, M. Sirinivas, D.S. Sarma, Effect of solution treatment temperature on microstructure and mechanical properties of hot isostatically pressed superalloy Inconel* 718. Mater. Sci. Technol. **20**, 1161 (2004)
17. W.C. Liu, F.R. Xiao, M. Yao, Z.L. Chen, Z.O. Jiang, S.G. Wang, Relationship between the lattice constant of Y phase and the content of δ phase, γ'' and γ' phases in Inconel 718. Scripta Mater. **37**(1), 59 (1997)
18. C. Slama, M. Abdellaoui, Structural characterization of the aged Inconel 718. J. Alloy. Compd. **306**, 277 (2000)
19. G. Muralidharan, R.G. Thompson, S.D. Walack, Analysis of precipitation in cast alloy 718. Ultramicroscopy **29**, 277 (1989)
20. P.J. Warren, A. Cerezo, G.D.W. Smith, An atom probe study of the distribution of rhenium in a nickel-based superalloy. Mater. Sci. Eng., A **250**, 88 (1998)
21. J.T. Goldstein, G. Ehrlich, Atom and cluster diffusion on Re(0001). Surf. Sci. **443**, 105 (1999)